The Journal of Neuroscience, February 1989, 9(2): 403–414

Passive Membrane Properties of Motorneurons and Their Role in Long-Distance Signaling in the Nematode *Ascaris*

Ralph E. Davis[1] and Antony O. W. Stretton[1,2]

[1]Neurosciences Training Program, and [2]Department of Zoology, University of Wisconsin–Madison, Madison, Wisconsin 53706

In the motornervous system of the large parasitic nematode, *Ascaris suum,* the dorsal and ventral nerve cords are connected by a repeating pattern of single identified motorneuron processes, called commissures (Stretton et al., 1978). By making microelectrode penetrations of the commissures, we here report the first successful intracellular recordings of nematode neurons. These cells, like muscle cells of *Ascaris,* exhibit resting potentials of approximately −30 to −40 mV. Several tests indicate that these are the normal resting potentials of the cells and are not low due to damage. Using 2 intracellular microelectrodes (one for stimulation and one for recording), we have determined the input resistance and cable properties of commissural motorneurons. Over the physiological voltage range, the steady-state *I–V* plots are linear with little indication that voltage-sensitive conductances are contributing substantially to signaling. The membrane capacitance is comparable to that of single biological membranes (range, 0.4–0.9 $\mu F/cm^2$) and the internal resistivity (range, 79–314 Ω cm) is similar to that found in other cells. Because of unusually large membrane resistances (range, 61–251 $k\Omega\ cm^2$), the space constants, λ, are high (range, 4–10 mm). Such membrane properties produce cells that are well-designed for conducting passive signals over long distances. This long-distance signaling ability appears to be due to the intrinsic properties of the motorneuron membrane itself.

For the analysis of the function of a nervous system, the nematode nervous system has several attractive features: The number of neurons is small, and the shape of individual neurons is simple and reproducible from animal to animal (Goldschmidt, 1908; White et al., 1976; Stretton et al., 1978; Walrond et al., 1985). Consequently, morphological studies on nematode nervous systems both in *Ascaris* and, to an even greater extent, in *Caenorhabditis elegans* have been carried out with a degree of completeness that is unusual, even among simple nervous systems. However, the properties of individual neurons are complex so that morphological studies alone are not sufficient to describe the way the nervous system works; direct recording of the electrical signals in each neuron is necessary. In this paper we describe the first successful intracellular electrical recordings from nematode neurons. These have been obtained from the large parasitic nematode *Ascaris,* in which the motorneurons are large enough to make such recordings feasible.

In nematodes the cell bodies of the motorneurons are located in the ventral nerve cord (Fig. 1). Although they are large (50 × 75 μm), they are not clustered into ganglia. Furthermore, the nerve cord is covered with a plexus of muscle arms, receiving neuronal input, so the cell bodies of the neurons are not visible; a satisfactory method of dissecting away the muscle tissue overlying the nerve cord has not yet been found. Our intracellular recordings were therefore made, not from the cell bodies, but rather from the commissures of the motorneurons (Figs. 1–3). The commissures are single fibers that link the dorsal and ventral branches of 5 of the 7 types of motorneurons, namely, the 3 types of dorsal excitatory motorneurons (DE1, DE2, and DE3), the dorsal inhibitory motorneuron (DI), and the ventral inhibitory motorneuron (VI; Fig. 3). It has been shown previously that the commissures occur in a repeating pattern that is reproducible from animal to animal, so the commissures of individual motorneurons can be recognized easily (Stretton et al., 1978; Johnson and Stretton, 1985; Walrond et al., 1985). On this basis, we have developed preparations in which microelectrode penetration of identified motorneurons can be carried out under visual control.

In this paper we have examined the membrane properties of the motorneurons and have found that, although the motorneurons transmit information over long distances, they do so by passive signaling rather than with propagated action potentials. Our measurements of the membrane properties of the neurons show that the membrane resistance is high and that this can account for such long-distance passive signaling. In the second paper of this series (Davis and Stretton, 1989), we extend our study to the nature of motorneuron signals and synaptic transmission.

Materials and Methods

Electrophysiological techniques. Standard electrophysiological techniques were used. Intracellular recordings from motorneuron commissures were made with 3 M KCl-filled microelectrodes (60–100 MΩ). In a number of experiments, 2 M KOAc-filled microelectrodes (80–120 MΩ) were used. Resting potentials, postsynaptic potential (PSP) amplitudes, responses to stimulation, etc., were indistinguishable for the 2 types of electrodes. Microelectrodes were connected to a recording system through preamplifiers equipped with bridge circuits that allow recording and current injection from the same microelectrode. The recording system consisted of a 4 channel oscilloscope run in parallel with

Received Nov. 9, 1987; revised July 18, 1988; accepted July 22, 1988.

We thank Drs. James Angstadt, Ching Kung, and Donata Oertel for critically reading the manuscript. We are also grateful to Dr. Carl Johnson and Judith Donmoyer for helpful discussions and to Ann Hallanger for providing micrographs from her unpublished work. The manuscript was capably typed by Mrs. Beth Davis. This work was supported by USPHS Grant AI 15429.

Correspondence should be addressed to Dr. Antony O. W. Stretton, Department of Zoology, Zoology Research Building, University of Wisconsin–Madison, Madison, WI 53706.

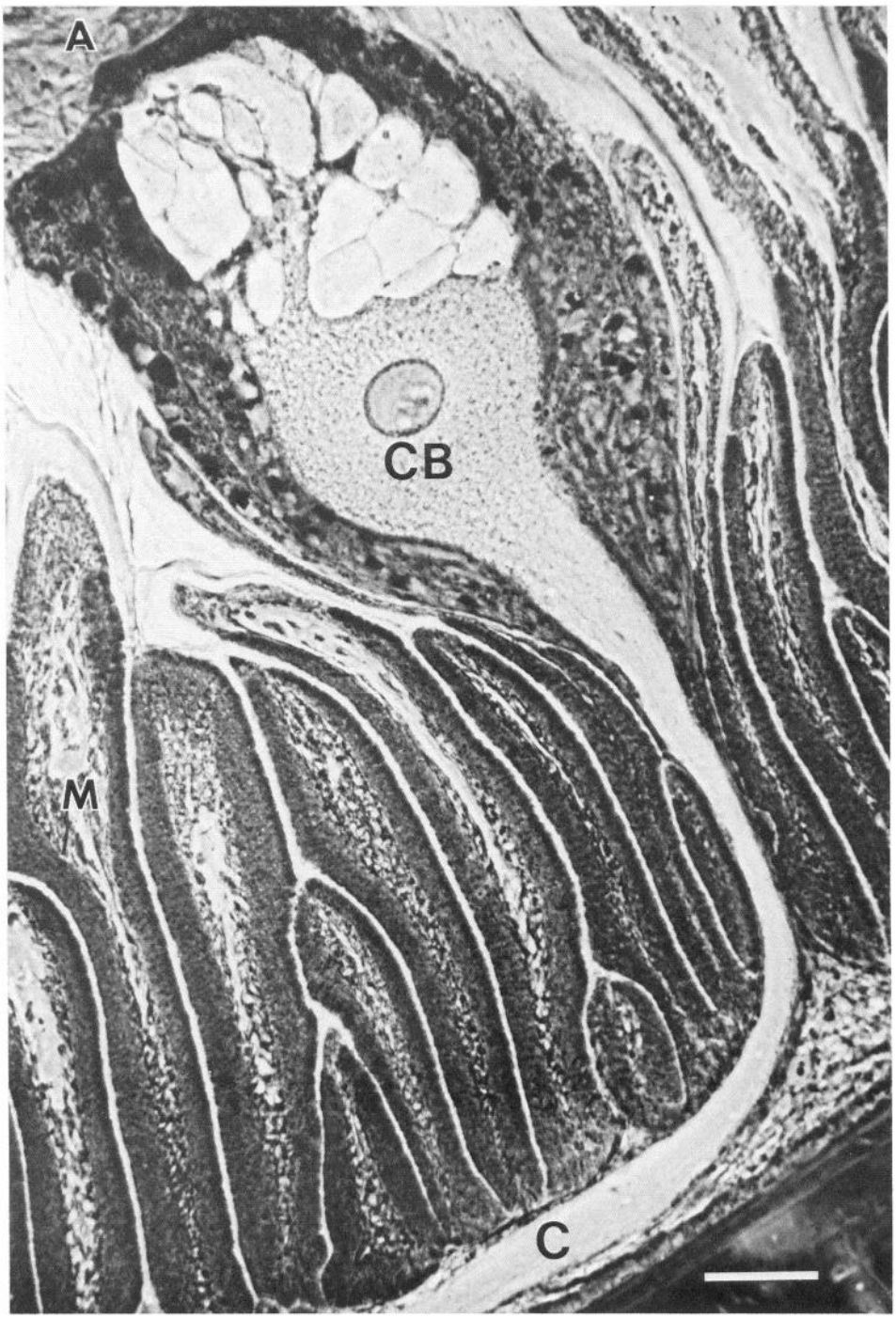

Figure 1. Cross section of the ventral nerve cord and surrounding muscle as seen in the light microscope. Neuronal profiles near the top of the field are packed together to form the ventral nerve cord and are supported by a closely apposed chalice of hypodermis. The large profile near the base of the neuronal profiles is the cell body (*CB*) of a commissural motorneuron. It sends out a process that travels within a thin layer of hypodermis underneath the muscle cells (*M*). This process, called a commissure (*C*), is the site of intracellular motorneuron recordings after overlying muscle has been removed. Muscle cells send processes called muscle arms (*A*) to the top of the nerve cord to receive their synaptic innervation from the neurons *en passant*. Scale bar, 30 μm.

paper chart recorders. In some experiments, data acquisition and analysis was computer assisted (pClamp software from Axon Instruments, Burlingame, CA). Externally applied current was measured with a virtual ground current monitor. Nerve cord processes of motorneurons were stimulated extracellularly through suction electrodes. Distance measurements between microelectrodes were made with a calibrated eyepiece.

Perfusion apparatus and salines. All of the electrophysiological experiments were carried out in a Sylgard-lined Plexiglas bath chamber (volume, 1.5 ml). Gravity-fed salines were perfused through a hot water jacket and then into the Plexiglas chamber such that a bath temperature of 37 ± 2°C was maintained. The flow rate of the saline was approximately 1.5 ml/min.

Ascaris saline contains 4 mM NaCl, 125 mM NaOAc, 24.5 mM KCl, 5.9 mM $CaCl_2$, 4.9 mM $MgCl_2$, and 5 mM TES (*N*-tris-[hydroxymethyl]methyl-2-aminoethane sulfonic acid) or Tris buffer, pH 7.4. In such a saline, which has an ionic composition similar to that of the pseudocoelomic fluid of the worm, muscle cells show spontaneous activity with graded spikes. This activity can be so pronounced as to produce massive muscle contractions, making it difficult to hold either muscle or motorneuron impalements for long periods. A modified saline containing twice the above concentrations of Ca^{2+} and Mg^{2+} (i.e., 11.8 mM $CaCl_2$ and 9.8 mM $MgCl_2$) was therefore used in these experiments. This reduces the spontaneous activity in muscles (Walrond et al., 1985) and allows stable recordings for prolonged periods. In Co^{2+}-containing saline, the $CaCl_2$ was replaced with $CoCl_2$.

The dissected preparation and electrode placement. Worms were obtained from the intestines of freshly killed pigs at a local slaughterhouse. In the laboratory they were maintained at 37°C in PBS (140 mM sodium chloride, 10 mM sodium phosphate, pH 7.0–7.5). In most experiments,

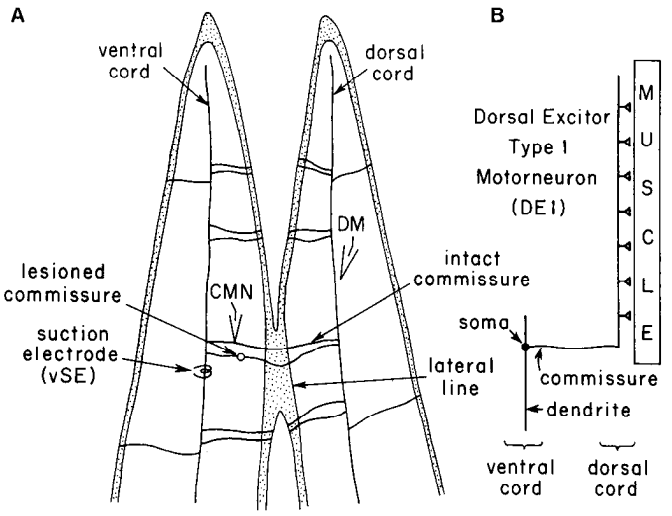

Figure 2. *A,* Diagram showing a dissected preparation used for recording from a single commissural motorneuron and muscle cells it innervates. See Materials and Methods for a description of how such a preparation is obtained. *B,* Diagram illustrating the different parts of a representative commissural motorneuron (in this case, a DE1) and the relationship of its processes to the nerve cords and muscle cells it innervates. *CMN,* commissural motorneuron; *DM,* dorsal muscle; *vSE,* ventral suction electrode.

large female worms, 25–30 cm long, were used. The commissures of single, uniquely identifiable motorneurons can be seen from the outside of the animal using a dissecting microscope and dark-field illumination. The particular commissure to be studied was marked by puncturing the cuticle with a Minutien pin dipped in carmine red particles on both sides of the commissure as it courses between the ventral and dorsal nerve cords. Commissures usually occur in pairs separated from one another by a few hundred micrometers (Fig. 2). For single-motorneuron studies, the unwanted member of the pair was commonly cut with a Minutien pin or an electrolytically sharpened tungsten needle. Excitatory and inhibitory motorneurons can be distinguished from one another on a combination of both anatomical [anterior/posterior position and commissural thickness (Johnson and Stretton, 1985)] and physiological grounds [sign of stimulated postsynaptic response (Stretton et al., 1978; Walrond et al., 1985)]. A piece of the worm, 3–5 cm long, including the complete motorneuron to be studied, was then taken from the animal; after cutting the lateral line that did not contain the commissure, the preparation was pinned out flat in the chamber with the muscles uppermost. The gut was removed with forceps. The lateral line through which the intact commissure passes was then cut both anterior and posterior to the marked commissure (Fig. 2*A*). These cuts severed all other connections between the ventral and dorsal nerve cords; therefore, generally, the bridge of tissue that included the single intact motorneuron was the only remaining connection between the dorsal and ventral halves of the animal (Walrond et al., 1985).

A mat of muscle cells overlies the thin hypodermal layer within which the commissure is found (Fig. 1). In the area of the tissue bridge, through which the single intact commissure is known to course, a small patch of muscle cells was removed with fine forceps from the hypodermis to which they attach. Muscle removal must be carried out with delicacy since the hypodermis intervening between the muscle cells and the commissure can be as little as 5–10 μm thick. With the muscle removed, the commissure could be seen within the translucent hypodermis and penetrated with a microelectrode under visual control.

The electrode placements were as follows. A microelectrode was placed in a muscle cell within the output zone of the motorneuron (Stretton et al., 1978; Walrond et al., 1985), to monitor synaptic output of the motorneuron. A second microelectrode was placed in the exposed commissure to record from the motorneuron intracellularly or to inject current. The motorneuron could be stimulated extracellularly by a suction electrode placed over the nerve cord where the motorneuron's dendrite courses. In some experiments, 2 microelectrodes were placed in the same commissure, one for intracellular stimulation and the other for intracellular recording.

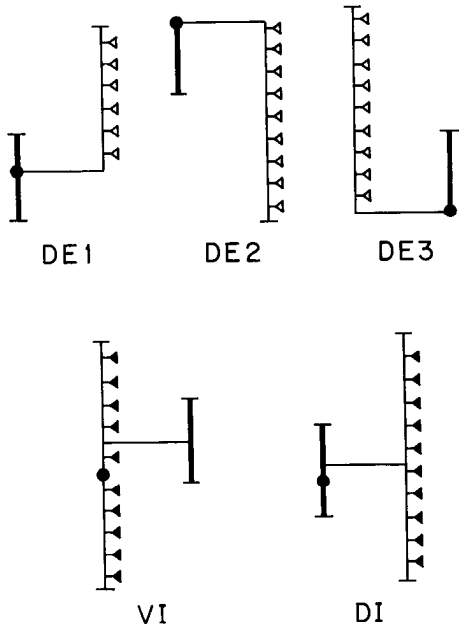

Figure 3. Diagram showing the functional morphology of the 5 types of commissural motorneurons in *Ascaris. Vertical lines* represent processes in the dorsal or ventral nerve cords, and *horizontal lines* represent commissures. *Dots* represent cell bodies that occur within the ventral nerve cord and serve to identify it. *Thick lines* show dendritic regions, and *triangles* represent axonal regions where synapses both to muscle cells and to other neurons are made. *Open triangles* indicate excitatory synaptic output, and *solid triangles* indicate inhibitory synaptic output.

Microscopic techniques. The light microscopic techniques used have been previously described (Stretton, 1976). Electron microscopy was carried out as follows. Portions of worms in which identified commissures had been marked with carmine particles as described above were fixed for 6 hr at 4°C. The fixative consisted of 3% glutaraldehyde/3% acrolein in 0.1 M phosphate buffer, pH 7.3. The worm pieces were further trimmed and then postfixed in 2% osmium tetroxide for 1.5 hr. The tissue was then *en bloc* stained with 1% uranyl acetate before being dehydrated and embedded in Epon resin. Thick sections (8 μm) of the hardened plastic were examined in the light microscope and appropriate sections were then removed and reembedded on dummy Epon blocks. Thin sections (70 nm) of the reembedded material were collected on copper grids and stained with a saturated uranyl acetate–ethanol solution followed by lead citrate. Stained sections were examined with a Hitachi HS-7S electron microscope.

Results

Resting potentials of commissural motorneurons

The resting potentials of the motorneurons range from −25 to −44 mV (Table 1). *Ascaris* muscle cells have similar resting potentials (del Castillo et al., 1964; Brading and Caldwell, 1971). Since these resting potentials are low compared with those obtained in neurons in many other systems, we wondered whether the neurons were damaged by the dissection procedure or by impalement.

While recording from a dorsal muscle cell postsynaptic to a DE1 neuron, the DE1 dendrite was stimulated with a brief suction electrode pulse. Dorsal muscle responses were recorded before removing the muscle patch overlying the commissure, after removing the patch to expose the commissure for penetration, and after impaling the commissure with a microelectrode (Fig. 4). The similarity of the dorsal muscle response before, during, and after these manipulations suggests that damage to the motorneuron due to the dissection or microelectrode impalement is minimal.

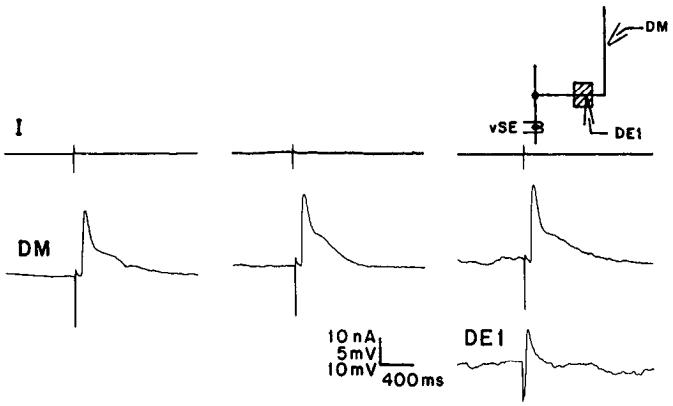

Figure 4. The commissural motorneuron is not significantly damaged by dissection or by microelectrode impalement. The intracellularly recorded dorsal muscle response (*DM*) to a brief current pulse (monitored in *top trace*) delivered by a ventral suction electrode (*vSE*; *left panel*) did not change after muscle removal (*center panel*), and after motorneuron penetration (*right panel*; intracellular response in DE1 shown in *bottom trace*). *Insets* in this and the following figures are schematics of the recording arrangements. *Hatching* in this inset (*top right*) represents region where muscle cells were removed to expose the commissure.

Monitoring membrane potential with successive microelectrode penetrations of a motorneuron also gives an indication of the extent to which damage can occur. This was of special importance because the experiments to determine motorneuron membrane constants described below involved several sequential penetrations. A series of 9 consecutive penetrations were made in the same DE1 motorneuron while recording intracellularly from a postsynaptic muscle cell. Penetrations 1, 5, and 9 are shown in Figure 5. There was a relatively small (6 mV) decline in resting potential over the course of the 9 penetrations. This particular DE1 motorneuron exhibited one of the largest initial resting potentials (−44 mV), suggesting that it is unlikely to have been significantly damaged by the first penetration. The spontaneous IPSPs, which typically occur in this class of motorneurons, and the low-amplitude background "noise" commonly seen in motorneurons were observed in the first penetration and remained relatively unchanged throughout the 9 successive penetrations. Intracellular current pulses of constant amplitude and duration were administered through the microelectrode, and the response in dorsal muscle was monitored for each of the consecutive penetrations (Fig. 5). The graded spikes evoked in dorsal muscle, though varying slightly from pulse to pulse, remained strong over the course of the multiple motorneuron penetrations. This result indicates that the ability of the motorneurons to activate muscle synaptically is not greatly affected by multiple microelectrode penetrations.

The following additional lines of evidence also suggest that the resting potentials observed in these cells do not reflect significant damage due to microelectrode penetration.

1. While recording from a motorneuron with one microelectrode, a second microelectrode can be inserted into the same cell (Fig. 6, *A, B*). Occasionally, a rapid, transient depolarization was monitored in the first microelectrode, but the resting potential usually stabilized to its previous level within a few seconds. More often, penetration with the second microelectrode resulted in no more than a 2–3 mV decrease in the resting potential as measured by the first microelectrode. In addition, PSPs occurring prior to the second penetration continue after that penetration seemingly unaffected in amplitude, duration, and shape.

2. While monitoring muscle membrane potential and spontaneous postsynaptic activity with one microelectrode, a penetration of a motorneuron innervating that muscle cell can be made. In early experiments with low-resistance microelectrodes (15–30 MΩ, 3 M KCl), impalement of an excitatory motorneuron usually resulted in a large long-lasting depolarization of the muscle cell upon which a number of muscle spikes were superimposed. The resting potential in these early experiments was almost always low (−5 to −15 mV). After optimizing the shape and resistance of the microelectrodes (60–100 MΩ, 3 M KCl), these discharges in muscle that are presumably the result of damage are rarely observed.

3. Stable recordings from motorneurons can be made for periods of up to 2 hr; spontaneous EPSPs or IPSPs (*cf.* Fig. 6) persist throughout this period. In contrast, with large-tipped, low-resistance electrodes, it is difficult to hold motorneurons for more than 10–15 sec.

4. We will show in the following paper that there is tonic release of neurotransmitter from motorneurons and that the relationship between neuronal membrane potential and postsynaptic muscle responses is approximately linear (Walrond et al., 1985; Davis and Stretton, 1989). Therefore, any significant change in the membrane potential of the neuron that is produced by microelectrode penetration should result in a change in the muscle membrane potential, yet little or no change was observed (Fig. 6*C*). Even low-amplitude depolarizing current injections (<0.5 nA) which change the presynaptic voltage by 2–4 mV, are capable of producing observable changes in postsynaptic membrane potential. The high sensitivity of these synapses to small changes in presynaptic voltage should make damage-induced depolarization of the presynaptic element readily detectable. Spontaneous activity present in muscle prior to penetration of the motorneurons is not noticeably affected by subsequent microelectrode penetration of a presynaptic neuron (Fig. 6*C*).

Passive spread along commissures

Simultaneous intracellular recordings from sites close to the ventral nerve cord and close to the dorsal nerve cord indicate

Table 1. Resting potentials for commissural motorneurons and muscle cells

Potential	DE1 (n = 10)	DE2 (n = 10)	DE3 (n = 4)	DI (n = 10)	VI (n = 10)	Muscle (n = 10)
Mean ± SD (mV)	35 ± 5	31 ± 3	33 ± 1	33 ± 4	33 ± 4	34 ± 4
Range (mV)	27–44	28–36	31–34	25–37	26–38	28–40
Median (mV)	35	31	33	34	34	34

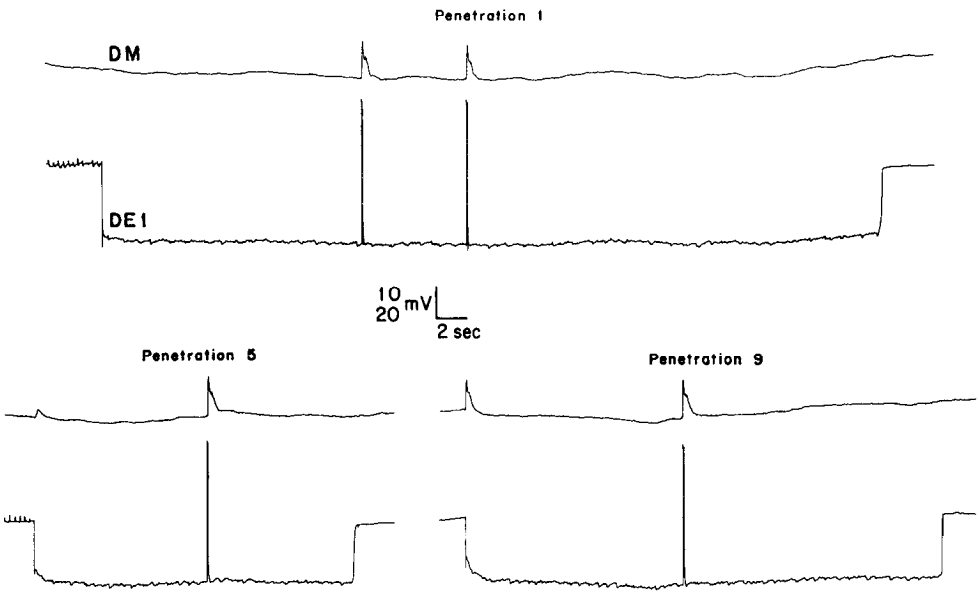

Figure 5. Multiple impalements of a commissure do not produce significant motorneuron damage as assayed by resting potential, dorsal muscle responses, or spontaneous PSP activity. While intracellularly monitoring dorsal muscle (*DM*), a DE1 was penetrated. DM responses were elicited by intracellular current pulses into the DE1 (2 nA, 75 msec; bridge circuitry unbalanced; current trace not shown). The DE1 microelectrode was then withdrawn. A series of similar penetrations, stimulations, and withdrawals was made. Of these penetrations, numbers *5* and *9* are also shown. The resting potential of the motorneuron declined from −44 to −38 mV over the course of the 9 penetrations. Comparison of the penetrations reveals little change in graded muscle spike responses or spontaneous PSP activity.

that spontaneous PSPs of ventral nerve cord origin can spread along the commissure (4–5 mm) with little decrement (Fig. 7). The amplitude of the ventrally recorded PSPs is larger than that recorded from the more dorsal microelectrode, suggesting that the PSPs originate ventrally. The PSPs persist even after the commissure is cut dorsally. Such PSPs can activate muscle 1.5 cm or more away from their site of origin (Fig. 7*B*). To understand the bases for this ability of signals to spread over long distances, the input resistance and cable properties of the commissural motorneurons were studied.

Input resistance

To determine the steady-state input resistance and cable properties of the DE1, DE2, DI, and VI motorneurons, 2 microelectrodes were inserted into each cell, one for stimulating and one for recording. Since the largest number of experiments were carried out on the DE1 motorneurons, the following results will focus on this class of neurons.

To determine the input resistance of DE1 neurons, the slopes of steady-state current–voltage relationships were measured. The

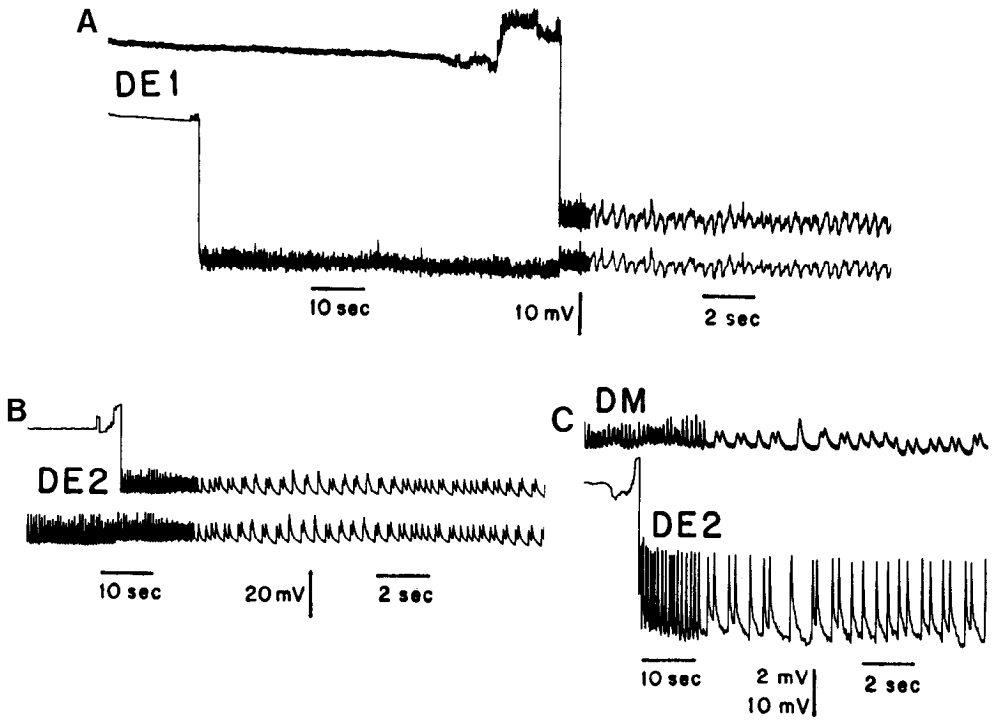

Figure 6. Microelectrode penetration has negligible effects on prior resting potential level and spontaneous PSP activity. *A,* Penetration of a DE1 motorneuron with one microelectrode (*lower trace*) was followed by subsequent penetration with a second microelectrode (*upper trace*) less than 25 μm away. The resting potential (as monitored by the first microelectrode) depolarized at most 2–3 mV at the time of the second microelectrode penetration. Spontaneous IPSPs continued as before the second penetration. Time axis changed as noted. *B,* While recording a DE2 motorneuron (*lower trace*), a second microelectrode (*upper trace*) penetrated the same cell. The membrane depolarized by 2–3 mV and EPSP activity continued as before the second penetration. Time axis changed as noted. *C,* While recording a dorsal muscle cell (*DM, upper trace*), a DE2 motorneuron was penetrated (*lower trace*; distance between recording sites, approximately 1 cm). The muscle resting potential remained unchanged, as did its DE2-induced PSP. Time axis changed as noted.

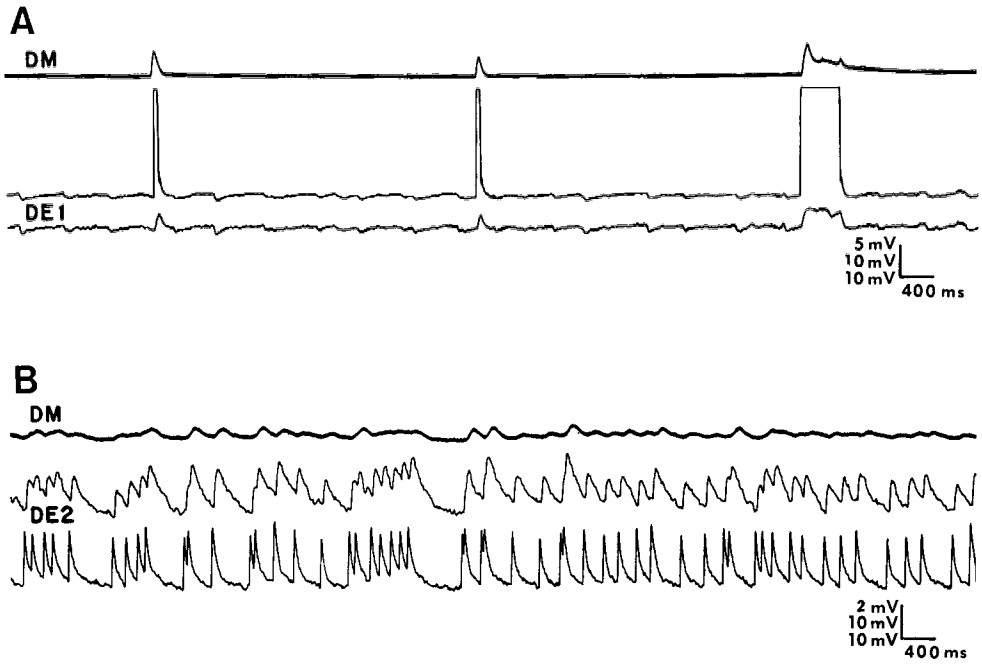

Figure 7. Spontaneous PSPs of ventral nerve cord origin can be conducted over long commissural distances with little decrement. *A,* Two microelectrodes approximately 4 mm apart simultaneously recorded from the same DE1 motorneuron (*2 lower traces*; the recording from the microelectrode closest to the ventral nerve cord is the *bottom trace* in *A* and *B*); intracellular records were also made from a dorsal muscle (*DM*) approximately 4 mm anterior to the entrance of the DE1 commissure into the dorsal nerve cord. Intracellular depolarizing current pulses (50 and 500 msec) were injected into one commissural microelectrode near the dorsal nerve cord (*middle trace*; bridge circuitry unbalanced). They produced electrotonic responses in the commissure and synaptic responses in dorsal muscle. Note that the size of the spontaneous IPSPs in DE1 decreased relatively little over the 4 mm distance between the 2 commissural microelectrodes. *B,* Two microelectrodes approximately 4.5 mm apart simultaneously recorded from the same DE2 motorneuron; a DM cell was penetrated approximately 1 cm posterior to the entrance of the DE2 commissure into the dorsal nerve cord. Note that the spontaneous EPSPs experienced little decrement over the 4.5 mm distance between the 2 commissural microelectrodes. The *upper trace* illustrates that these EPSPs are effective in producing DM responses approximately 1.45 cm away from their origin in the ventral nerve cord.

average input resistance was 7.1 ± 1.9 MΩ (range, 5–12 MΩ, n = 10; Fig. 8). The graph is nearly linear between −5 and +5 nA of injected current, corresponding to voltage changes of between about −40 and +40 mV, the physiological voltage range of these cells. Above and below those current values, the points show increasing scatter, possibly the result of the erratic current-passing characteristics of high-resistance microelectrodes. The linearity of the plots indicates that a significant rectifying current does not occur in the commissures of these cells.

On occasion, injection of strong depolarizing currents produced a small onset transient indicative of a voltage-sensitive response (see Fig. 9, *A, C,* arrows). This peak is small (<5 mV for steady-state voltage changes of +40 to +50 mV) and graded with current strength; the *I–V* plot of the peak response differs only negligibly from that of the steady state. This peak response is reversibly blocked by Co^{2+} (Fig. 9). We have obtained *I–V* plots before, during, and after perfusion with such a Co^{2+} saline. As shown in Figures 9 and 10, there was only a slight change in the steady-state input resistance before (5.5 MΩ), during (5.1 MΩ), and after the Co^{2+} perfusion (5.2 MΩ). The absence of a significant change in the steady-state portion of the potential during perfusion with Co^{2+} saline suggests that Co^{2+}-blockable, voltage-sensitive channels do not have a substantial amplifying effect on steady-state signal conduction across the DE1 commissure.

The DE2, DI, and VI motorneurons have linear *I–V* plots for hyperpolarizing and relatively weak depolarizing current pulses (Fig. 11); in contrast to the excitatory motorneurons, strong depolarizing pulses elicit rhythmic oscillatory potentials in inhibitory neurons (see further description in Davis and Stretton, 1989). Activation of these voltage-sensitive responses by depolarization prevents one from obtaining complete steady-state *I–V* plots for the inhibitors. The linear portions of the *I–V* plot were used to determine the input resistance and cable properties of all neurons studied.

Long-distance passive signaling: cable properties

Figures 12 and 13 show the results of experiments to measure the passive spread of voltage changes in motorneurons. Traces from experiments involving an excitatory motorneuron (DE1; Fig. 12) and an inhibitory motorneuron (VI; Fig. 13) are illustrated. Cells were impaled with 2 microelectrodes. The amplitude of the voltage change decrements with increasing distance from the stimulating microelectrode for a constant-current pulse.

In the case of the DE1 neuron (Fig. 12), it was possible to return to the zero separation position at the end of the experiment. The second measurement at zero separation gave a voltage response that was comparable to (in fact, slightly larger than) the initial value. This result indicates that the commissure had not been significantly damaged over the course of the multiple penetrations made along its length.

The slope of plots of ln voltage versus distance, determined by regression analysis, was used to calculate the cable constants, including λ, shown in Table 2 using the equations that describe an infinitely long cable. Using the equation $V_x = V_o e^{-x/\lambda}$, where

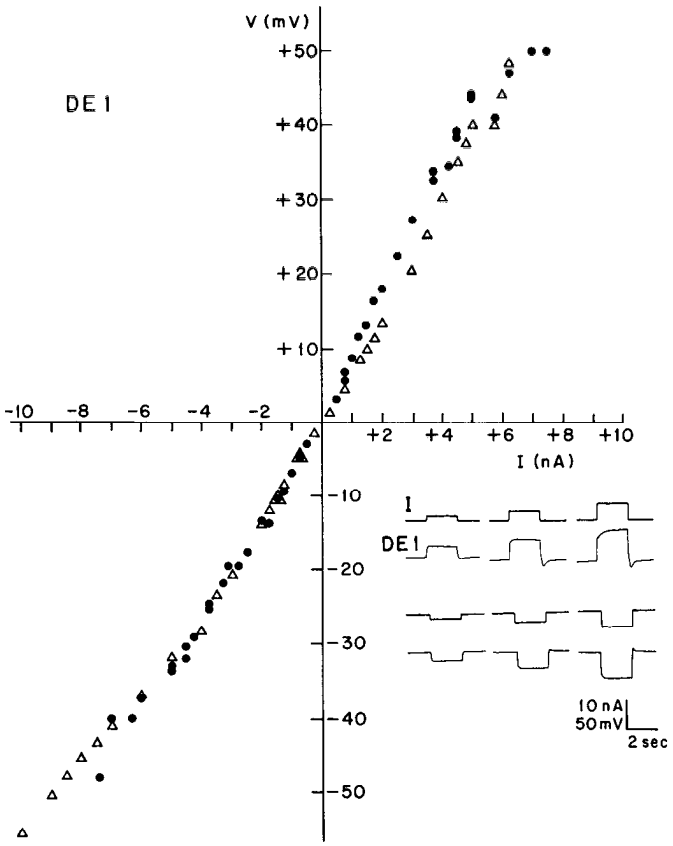

Figure 8. *I–V* plots of 2 DE1 motorneurons determined with 2 microelectrodes (one for stimulating, one for recording). The intersection of the axes marks the resting potential, −34 (△) and −36 mV (●). *Insert* shows representative traces for one of the experiments (●).

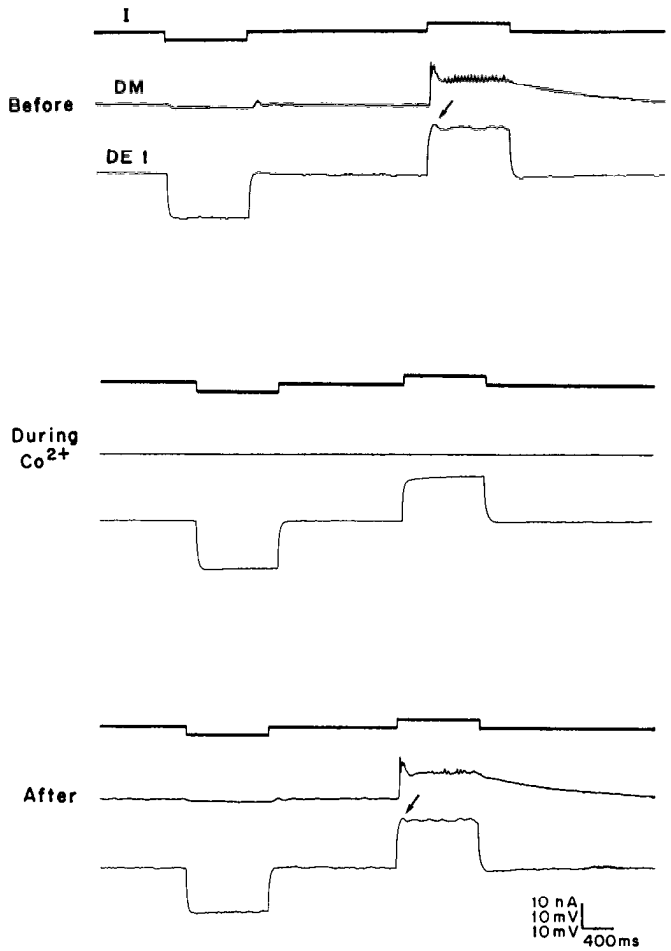

Figure 9. Sample records of data used to construct the *I–V* plots seen in Figure 10 before, during, and after the Co^{2+} saline perfusion. The upper trace (*I*) is the current monitor. The middle trace (*DM*) is an intracellular recording of a dorsal muscle cell. The lower trace (*DE1*) is an intracellular recording of the voltage change induced by current injection from a stimulating microelectrode. Muscle responses to hyperpolarizing current pulses show that motorneurons release neurotransmitter tonically at their normal resting potential (see Davis and Stretton, 1989). The disappearance of the synaptically evoked dorsal muscle response can be used as an assay for completeness of Co^{2+} block.

$V_o = (I/2)\sqrt{r_m r_i}$, we obtained the effective resistance ($\sqrt{r_m r_i}$). From the effective resistance, the R_{input} ($\sqrt{r_m r_i}/2$) at the zero point was calculated in cable property experiments. The average R_{input} thus obtained in the 10 DE1 experiments of Table 2 is 6.0 ± 1.5 MΩ (range, 5–10 MΩ). This value is consistent with the value obtained (in separate experiments) from the calculated slopes of *I–V* plots mentioned above (7.1 ± 1.9 MΩ; range, 5–12 MΩ). DE1 motorneurons possess an internal resistivity (average R_i = 79 Ω cm²) similar to that found in many other excitable cells. The specific membrane resistivity (average R_m = 69 kΩ cm²) is unusually high and accounts for the large space constants (average λ = 8 mm) of these cells. The membrane time constant (average τ_m = 32 msec) is also somewhat higher than that found for most cells. Membrane capacitance values (average C_m = 0.5 μF/cm²) are close to the values obtained for most unit biological membranes.

For 2 DE1 neurons cable property analysis was carried out using both depolarizing and hyperpolarizing current pulses. Within each experiment, there was very close agreement between the membrane constant values determined by either depolarizing or hyperpolarizing currents (depolarizing/hyperpolarizing: R_m, 46/40, 77/73 kΩ cm²; λ, 5/6, 8/8 mm). In 3 non-DE1 experiments (1 DI, 2 VIs) variation within each experiment was greater, but it was not systematic (depolarizing/hyperpolarizing: R_m, 180/262, 390/203, 336/387 kΩ cm²; λ, 11/15, 14/9, 9/11 mm). Within an experiment, the relative similarity of depolarizing versus hyperpolarizing values suggests (as do the linear *I–V* plots) that active conductances are not making significant contributions to the steady-state voltage changes.

In Figure 14, comparisons were made between the time course of the responses at zero electrode separation and the theoretical curves calculated from the error function (Hodgkin and Rushton, 1946). For the DE1 motorneuron shown in column A, the time course of the rise and fall closely approximated the theoretical curve, indicating that this neuron was behaving purely passively. A similarly close approximation is seen for hyperpolarizations in a VI motorneuron shown in column B; however, small onset and offset deviations from the predicted curve occurred for strong depolarizations, indicating the presence of weak active responses. These are discussed further in Davis and Stretton (1989). The contribution of the active channels varies considerably between individual neurons of the same cell type and between the same identified neuron from different animals; in some cases, the channels seem to be absent, and in others they are clearly present.

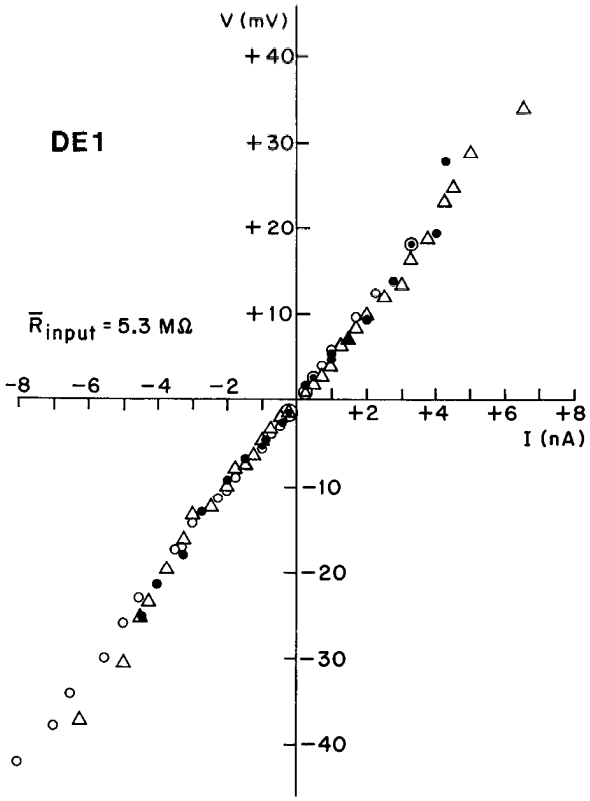

Figure 10. *I–V* plots obtained from a DE1 motorneuron in successive perfusions of high Ca^{2+} saline (○), Co^{2+} saline (△), and Ca^{2+} saline again (●). Successive input resistances were 5.5 MΩ (○), 5.1 MΩ (△), and 5.2 MΩ (●). The intersection of the axes marks the resting potential level, −32 to −35 mV.

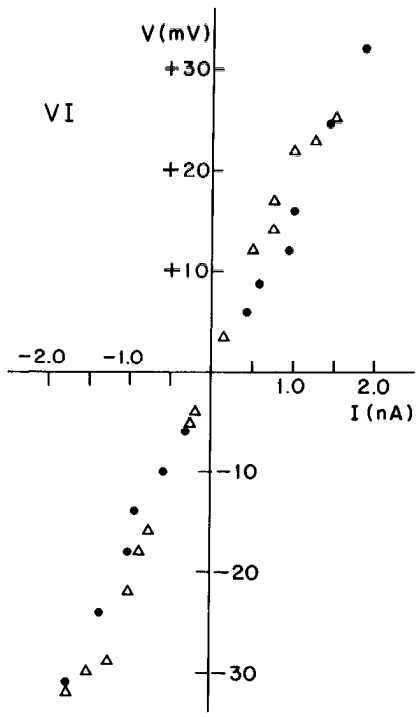

Figure 11. *I–V* plots for 2 different VI motorneurons. Input resistances were 15 (●) and 20 MΩ (△). The intersection of the axes marks the resting potential level, −31 (●) and −30 mV (△). Active responses in the form of oscillating potentials occurred for depolarizing steps above 1.5–2 nA of injected current (see Davis and Stretton, 1989).

Electron microscopy

Electron microscopy has been carried out on cross sections of commissures. The commissure is surrounded by a loose wrapping of hypodermal membranes and portions of hypodermis they enclose (Fig. 15, *A, B*). The hypodermal membranes are on the order of 10–12 nm in thickness. The number of membrane-enclosed layers is small, varying from 1 to 7; each layer ranges from 70 to 200 nm in width. The membrane wrappings, unlike those of myelin, have frequent discontinuities (Fig. 15*B*). The width of the extracellular space ranges between 15 and 300 nm. The extracellular space between the commissural membrane and the innermost hypodermal membrane is approximately 50 nm with the distance to the outermost hypodermal membrane being <3 μm. One possible explanation for the high membrane resistivities is that occlusions in the extracellular space increase the shunt resistance. Examination of the wrappings, however, has yielded no evidence of structures that might produce such occlusions. The following considerations suggest that the observed membrane resistivity is intrinsic to the neuronal membrane and is not due to impeded ion flow around the commissure:

1. Anatomically, tightly adherent myelin-like wrappings or junctions occluding extracellular space are not present.
2. Physiologically, a C_m (0.4–0.9 μF/cm²) close to the value obtained for a single biological membrane suggests that the large R_m reflects a property inherent in the commissural membrane itself.

Table 2. R_{input} and cable properties of DE1, DE2, DI, and VI motorneurons

	DE1 (n = 10)		DE2 (n = 3)		DI (n = 3)		VI (n = 3)	
Parameter	Mean ± SD	Range	Mean ± SD	Range	Mean ± SD	Range	Mean ± SD	Range
R_{input} (MΩ)	6 ± 1.5	5–10	11 ± 2.3	10–14	15 ± 5.3	8–22	17± 5.0	12–22
R_i (Ω cm)	79 ± 29	37–118	314 ± 171	156–496	166 ± 46	118–209	157 ± 29	140–190
R_m (kΩ cm²)	69 ± 27	35–107	61 ± 16	51–81	214 ± 110	100–320	251 ± 119	163–387
λ (mm)	8 ± 2.6	5–13	4 ± 1.7	3–6	9 ± 5	5–15	10 ± 1.2	9–11
τ_m (msec)	32 ± 7.7	25–49	59 ± 18	46–72	92 ± 43	56–140	90 ± 22	66–109
	(n = 9)		(n = 2)					
C_m (μF/cm²)	0.5 ± 0.3	0.3–0.9	0.9	0.9	0.5 ± 0.1	0.4–0.6	0.4 ± 0.2	0.3–0.6
	(n = 9)		(n = 2)					

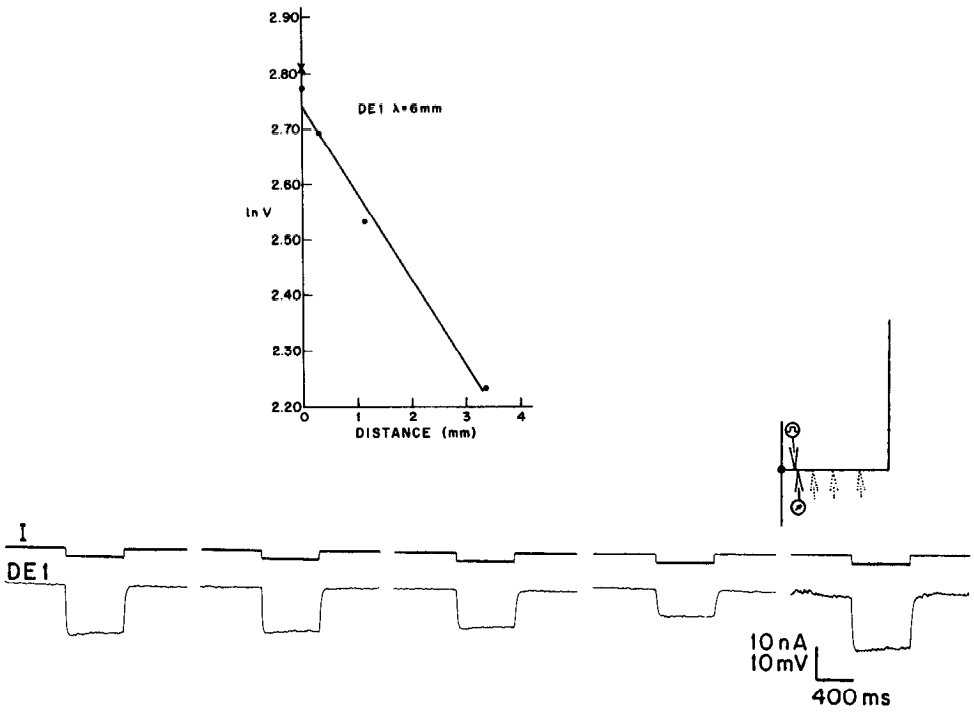

Figure 12. Space constant (λ) determined from ln V versus distance plot (via regression analysis) for a DE1 motorneuron. The current monitor (I) records the constant-amplitude hyperpolarizing current pulse injected by a stimulating microelectrode. The DE1 trace records the voltage decrement that occurred in response to this current at the following interelectrode distances (*left to right*): zero separation, 0.3, 1.1, 3.4 mm, and zero separation again (× marks the second zero separation point in the plot).

Comparison of input resistance and cable properties among different classes of motorneurons

Table 2 lists the input resistance and cable properties for 4 of the 5 classes of motorneurons: DE1, DE2, DI, and VI. Because of the small diameter of the DE3 neuron (<15 μm), it has not yet been possible to determine DE3 cable properties.

Two I–V plots for DE2 motorneurons yield input resistances (11, 12 MΩ) consistent with those obtained from cable equations (11 MΩ). Three I–V plots for VI motorneurons have also yielded input resistances (15, 20, and 24 MΩ) consistent with the table value (17 MΩ). These congruencies suggest that a representative sampling of the non-DE1 cells has been obtained.

Discussion

Resting potentials of motorneurons

Since the resting potentials of motorneurons are low (−30 to −40 mV) compared with those in many other organisms, var-

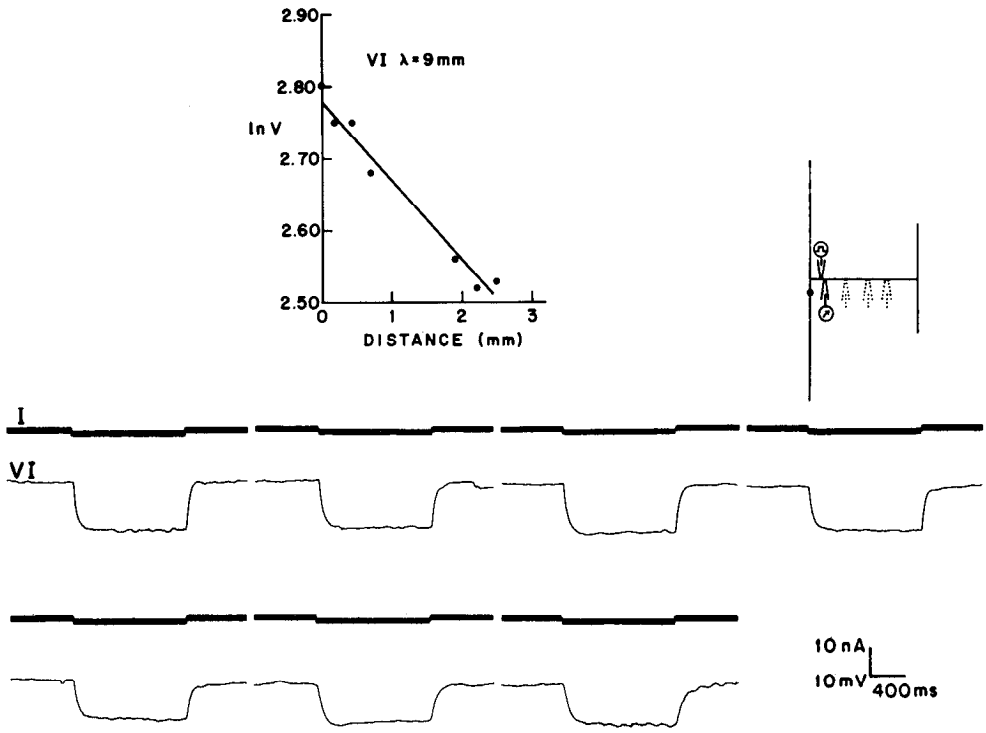

Figure 13. Space constant (λ) determined from ln V versus distance plot (via regression analysis) for a VI motorneuron. The VI trace records the voltage decrement that occurred in response to constant current pulses applied at the following interelectrode distances (*left to right*): zero separation, 0.2, 0.4, 0.7, 1.9, 2.2, and 2.5 mm.

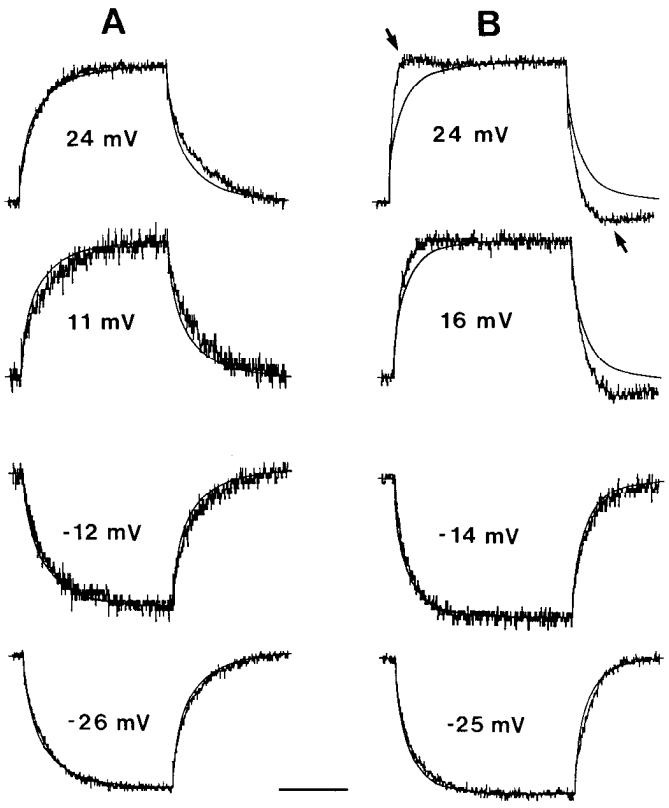

Figure 14. Experimental and theoretical curves showing the rise and fall of voltage in response to different levels of injected current. Two electrodes were placed in a DE1 motorneuron (*A*) or a VI motorneuron (*B*) at approximately zero separation. Depolarizing and hyperpolarizing current pulses were given. Steady-state values for the experimental voltage steps that result are indicated with respect to the resting potential (−33 mV for both cells). Theoretical curves (the nonnoisy lines) were determined using the τ_m for each cell (29 msec for DE1; 95 msec for VI) measured at 84% of final amplitude and the value of the error function tabulated from Table 1 of Hodgkin and Rushton (1946). Close agreement between experimental and theoretical curves is seen for all of the DE1 records and for the hyperpolarizations of the VI. The presence of weak active onset and offset components causes deviation between experimental and theoretical curves for strong depolarizations of the VI (*arrows*). The steady-state voltages of the experimental curves were normalized to the theoretical curves. Time scale bar, *A*, 50 msec; *B*, 250 msec.

ious experiments were designed to test whether damage due to dissection or microelectrode impalement was responsible. This was necessary to justify further analysis of the cable and other properties of these cells. The results of these experiments indicate that the motorneurons are not significantly damaged by dissection or microelectrode penetration.

Pearson (1976) has noted in his review of nonspiking neurons that such cells are commonly characterized by low resting potentials. This is often true of nonspiking cells that tonically release neurotransmitter (see Pearson and Fourtner, 1975; Burrows and Siegler, 1978; Siegler, 1985). *Ascaris* motorneurons fall into this category (Davis and Stretton, 1989).

Long-distance passive signaling: input resistance

Commissures of motorneurons are able to conduct PSPs over long distances to evoke postsynaptic responses a centimeter or more away. To determine whether this ability results from passive spread or whether it is aided by signal amplification through voltage-sensitive channels, measurements of the input resistance have been made.

Steady-state *I–V* plots are approximately linear over the physiological voltage range. The plots lack the changes in slope that would be indicative of significant voltage-sensitive conductances. Thus, it is unlikely that voltage-sensitive amplification is contributing substantially to the signaling ability of DE1 motorneurons. Voltage-sensitive channels exist in motorneuron membranes as revealed by the small Co^{2+}-blockable onset transient that can be elicited by strong depolarizing current pulses. However, steady-state input resistance does not change significantly when these channels are blocked with Co^{2+} saline.

Two considerations are in order. First, it is not possible to rule out completely the presence of depolarizing voltage-sensitive channels that are insensitive to Co^{2+} block. However, *Ascaris* motorneurons give no evidence of classical, fast action potentials, nor of the presumed voltage-sensitive Na^+ channels responsible for them (Davis and Stretton, 1989). In addition, Co^{2+} saline blocks depolarizing voltage-sensitive responses without revealing any significant underlying non-Co^{2+}-sensitive conductances. Second, though signal amplification may play little or no role in signal conduction in the commissure, its occurrence in the nerve cord processes of motorneurons would be expected, especially in output processes, due to the presence of voltage-sensitive conductances associated with synapses. No data is yet available on the signaling properties of nerve cord processes.

Both the excitatory and inhibitory motorneurons are capable of signaling over long distances. The linear steady-state *I–V* plots of the excitors suggest that they primarily rely on passive signaling of information. The inhibitors, on the other hand, while capable of long-distance passive signaling, are not merely passive cells. They, unlike the excitors, can generate oscillatory potentials (Davis and Stretton, 1989). Thus, in addition to their passive properties, these voltage-sensitive properties may also play a role in the signaling of the inhibitors.

Long-distance passive signaling: cable properties

The cable constants shown in Table 2, reveal that the 2 inhibitory motorneurons (DI and VI) exhibit higher R_m, R_{input}, and τ_m values than the excitatory motorneurons, DE1 and DE2. The difference in R_m between inhibitory and excitatory motorneurons is particularly striking, >200 kΩ cm² for inhibitors and <100 kΩ cm² for excitors. Inhibitory motorneuron processes have smaller diameters than DE1 and DE2 excitatory motorneurons: 10–25 μm for inhibitors and 20–35 μm for DE1 and DE2 excitors. Since λ is directly proportional to the square root of the diameter, if the membrane properties of inhibitors and excitors were the same, the inhibitory motorneurons would experience a greater passive signal decrement per unit distance. However, both excitatory and inhibitory motorneurons convey information over comparable distances. The increased membrane resistivity of inhibitory motorneurons may compensate for their smaller diameters, so that λ for both excitors and inhibitors is similar. Inhibitors also have a branched output process, whereas excitors do not (see Fig. 3). Again, a compensatory increase in R_m might allow the inhibitor to overcome the increased electrotonic decrement associated with a branch point.

Examination of Table 2 reveals that all of the motorneuron classes studied to date are characterized by R_i and C_m values that are comparable to those obtained for most nonmyelinated excitable cells in other nervous systems. Unlike cells in other

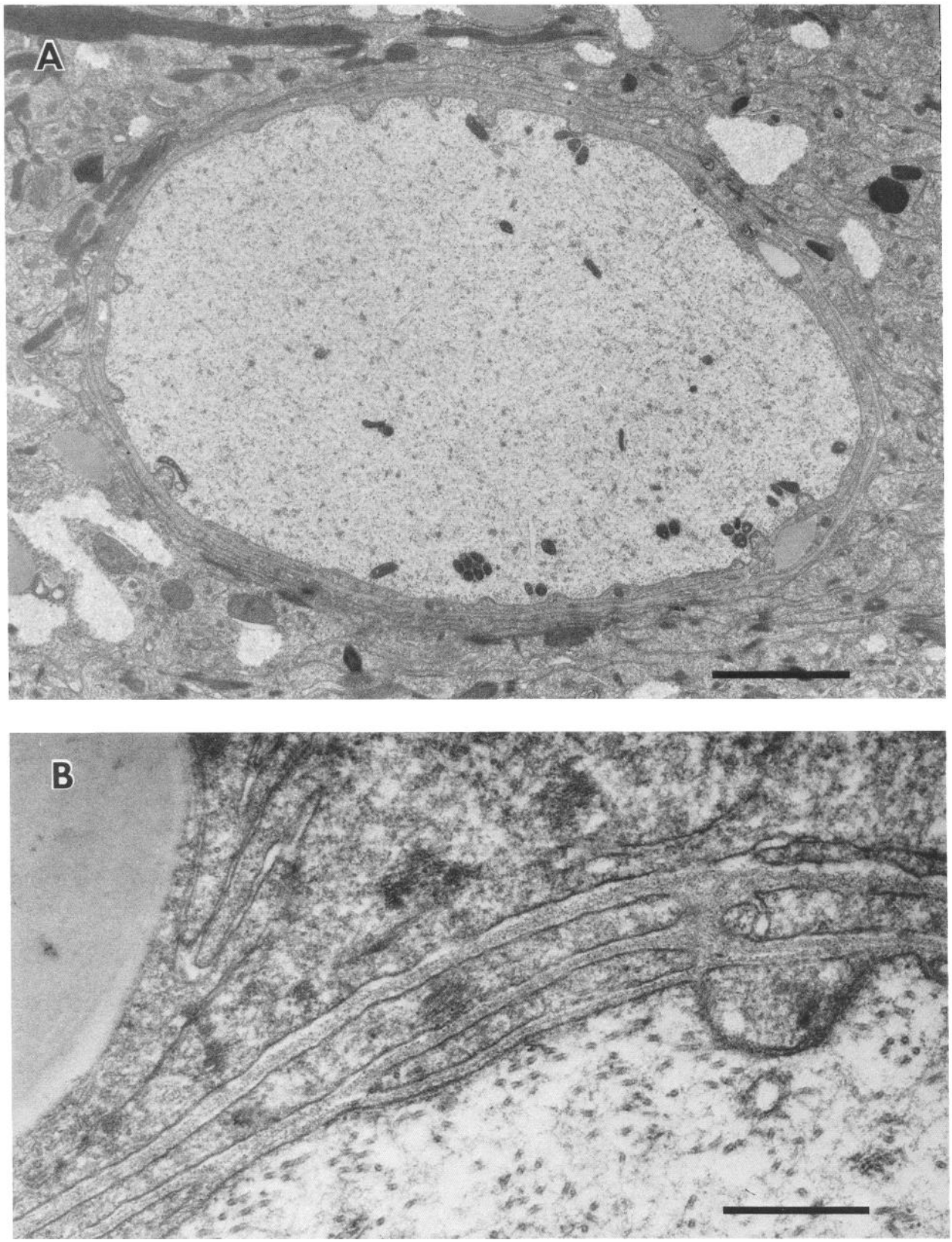

Figure 15. *A*, Electron micrograph of cross section of DE2 commissure (*C*). *B*, Note the discontinuous loose wrapping of hypodermal membranes adjacent to the commissure. Micrographs kindly provided by A. E. Hallanger. Scale bar: *A*, 2 μm; *B*, 0.5 μm.

systems (see Table 1 in Rall, 1977), *Ascaris* motorneurons exhibit unusually high values for R_m, λ, and τ_m. It is these properties that account for the observed ability of *Ascaris* motorneurons to use passive signals effectively over long distances.

As seen in Figures 8, 9, and 14*B* of this paper and documented more fully in the following paper (Davis and Stretton, 1989), these cells are capable of generating small transient depolarizing and hyperpolarizing active responses at either the onset or offset of injected current pulses. Though the conductances underlying them are too small to produce regenerative, full-blown action potentials, it is possible that the apparent long space constants of these cells may arise to some small extent from these conductances and not entirely from a high, strictly passive resistance. The linearity of our steady-state *I–V* curves indicate that these conductances are small and transient and therefore are, at best, only a very minor factor in determining the cable properties of these cells.

Such active conductances can, however, make determination of the time constant (from the rising or falling phase of the voltage response) somewhat uncertain. It is quite likely that the time constant has been underestimated in cells where such active conductances do produce slight onset or offset transients (as in the slight initial undershoot of Fig. 12, though not apparently in Fig. 13; *cf.* Fig. 14). Since our value for membrane capacitance is calculated from the time constant, it too will be underestimated. This may account for the slightly lower C_m values we obtained (0.4–0.9 μF/cm^2) in contrast to the 1 μF/cm^2 value found for most biological membranes. While there is an exponential decay of the electrotonic potential with distance, the rise or fall time of signals may be somewhat enhanced by the small active conductances in these otherwise passively signaling cells. Such a phenomenon is not without precedent (e.g., Detwiler et al., 1978) and may serve to maintain the sharpness of the onset and offset of PSPs conducted across the commissure.

Since synaptic activity can produce changes in membrane conductance, the effect of spontaneous PSP inputs onto motorneurons must be considered in determining cable properties. When the PSPs are blocked in Co^{2+} saline, no change in input resistance occurs, suggesting that synaptically induced conductances do not make a major contribution to the membrane properties. Furthermore, in *Ascaris* motorneurons, the periodicity of the spontaneous PSPs is low enough that during long current pulses, steady-state voltages can be measured between PSPs. In some preparations normal PSP activity is diminished or absent, yet the resting potential remains in the -30 to -40 mV range. Depolarizing or hyperpolarizing current pulses injected into the motorneurons do not reveal additional synaptic inputs, indicating that the resting potential is not at the equilibrium potential for PSPs. Furthermore, cable properties of cells with and without PSPs do not differ significantly.

A number of other organisms possess cells with unusual membrane properties, such as those seen for *Ascaris* motorneurons. Of particular interest are those with long neural processes like *Ascaris* motorneurons. The barnacle photoreceptor membrane has an R_m of 300 kΩ cm^2 and a λ of 10–18 mm (Hudspeth et al., 1977). Its high R_m, like that of *Ascaris* motorneurons, appears to be an intrinsic property of the receptor membrane. Unlike *Ascaris* motorneurons, it exhibits dramatic rectification in the depolarizing portion of its *I–V* plot. The cable properties of the coxal stretch receptor neurons of the crab *Carcinus* have been described (Bush, 1976; Cannone and Bush, 1980); these fibers have λ's of 10–20 mm. Pasztor and Bush (1982) have determined the cable properties of 3 mechanoreceptor neurons in the lobster; these cells have λ's (7–10 mm) and R_m's (100 kΩ cm^2) similar to those reported here for *Ascaris*. In studies to date, cells with long processes and such unusual membrane properties have characteristically been sensory cells which convey information that is graded with membrane potential. This study shows that motorneurons that convey graded signals may also make use of these properties and are thus capable of conveying passive signal information over centimeter distances.

References

Brading, A. F., and P. C. Caldwell (1971) The resting membrane potential of the somatic muscle cells of *Ascaris lumbricoides*. J. Physiol. (Lond.) *217:* 605–624.

Burrows, M., and M. V. S. Siegler (1978) Graded synaptic transmission between local interneurones and motor neurones in the metathoracic ganglion of the locust. J. Physiol. (Lond.) *285:* 231–255.

Bush, B. M. H. (1976) Non-impulsive thoracic-coxal receptors in crustaceans. In *Structure and Function of Proprioceptors in the Invertebrates,* P. J. Mill, ed., pp. 115–151, Chapman and Hall, London.

Cannone, A. J., and B. M. H. Bush (1980) Reflexes mediated by non-impulsive afferent neurones of thoracic-coxal muscle receptor organs in the crab, *Carcinus maenas*. 2. Reflex discharge evoked by current injections. J. Exp. Biol. *86:* 305–331.

Davis, R. E., and A. O. W. Stretton (1989) Signaling properties of *Ascaris* motorneurons: Graded active responses, graded synaptic transmission, and tonic transmitter release. J. Neurosci. *9:* 415–425.

del Castillo, J., W. C. de Mello, and T. Morales (1964) Influence of some ions on the membrane potential of *Ascaris* muscle. J. Gen. Physiol. *48:* 129–140.

Detwiler, P. B., A. L. Hodgkin, and P. A. McNaughton (1978) A surprising property of electrical spread in the network of rods in the turtle's retina. Nature *274:* 562–565.

Goldschmidt, R. (1908) Das Nervensystem von *Ascaris lumbricoides* und *megalocephala* I. Z. Wiss. Zool. *90:* 73–136.

Hodgkin, A. L., and W. A. H. Rushton (1946) The electrical constants of a crustacean nerve fiber. Proc. R. Soc. London [Biol.] *133:* 444–479.

Hudspeth, A. J., M. M. Poo, and A. E. Stuart (1977) Passive signal propagation and membrane properties in median photoreceptors of the giant barnacle. J. Physiol. (Lond.) *272:* 25–43.

Johnson, C. D., and A. O. W. Stretton (1985) Localization of cholineacetyltransferase within identified motoneurons of the nematode *Ascaris*. J. Neurosci. *5:* 1984–1992.

Pasztor, V. M., and B. M. H. Bush (1982) Impulse-coded and analog signaling in single mechanoreceptor neurons. Science *215:* 1635–1637.

Pearson, K. G. (1976) Nerve cells without action potentials. In *Simpler Networks and Behavior,* J. C. Fentress, ed., pp. 99–110, Sinauer, Sunderland, MA.

Pearson, K. G., and C. R. Fourtner (1975) Non-spiking interneurons in the walking system of the cockroach. J. Neurophysiol. *38:* 33–52.

Rall, W. (1977) Core conductor theory and cable properties of neurons. In *Handbook of Physiology,* Vol. 1, Section 1, E. R. Kandel, ed., pp. 39–97. Am. Physiol. Soc., Bethesda, MD.

Siegler, M. V. S. (1985) Nonspiking interneurons and motor control in insects. Adv. Insect Physiol. *18:* 249–304.

Stretton, A. O. W. (1976) Anatomy and development of the somatic musculature of the nematode *Ascaris*. J. Exp. Biol. *64:* 773–788.

Stretton, A. O. W., R. M. Fishpool, E. Southgate, J. E. Donmoyer, J. P. Walrond, J. E. R. Moses, and I. S. Kass (1978) Structure and physiological activity of the motorneurons of the nematode *Ascaris*. Proc. Natl. Acad. Sci. USA *75:* 3493–3497.

Walrond, J. P., I. S. Kass, A. O. W. Stretton, and J. E. Donmoyer (1985) Identification of excitatory and inhibitory motorneurons in the nematode *Ascaris* by electrophysiological methods. J. Neurosci. *5:* 1–8.

White, J. G., E. Southgate, J. N. Thomson, and S. Brenner (1976) The structure of the ventral nerve cord of *Caenorhabditis elegans*. Phil. Trans. R. Soc. London (Biol.) *275:* 327–348.